2014 IEEE/RSJ International Conference on
Intelligent Robots and Systems (IROS 2014)
September 14-18, 2014, Chicago, IL, USA

The Effect of Leg Impedance on Stability and Efficiency in Quadrupedal Trotting

William Bosworth[1], Sangbae Kim[1], and Neville Hogan[1,2]

Abstract— **Numerous legged robots have demonstrated the effectiveness of tuned leg impedance to achieve dynamically stable running and hopping. However, selecting appropriate impedance values for new machines remains challenging. This paper investigates the effect of joint impedance selection on locomotion stability and efficiency by analyzing a simulation model of the MIT Cheetah quadruped robot performing a trot gait. An exhaustive search of impedance parameters of the knee and hip shows that locomotion stability is highly sensitive to knee impedance and insensitive to hip impedance. Inspection of simulations operating during a ground-height disturbance reveals why: During a disturbance response most of the variation in work performed in the legs occurs in the knee joints. Mechanical work data from the MIT Cheetah exhibits close experimental agreement with the simulation predictions. The exhaustive search also reveals that, within the range of impedance parameters that can achieve stable locomotion, joint impedance values do not have a significant effect on the mechanical cost of transport. These results indicate that the dynamic response of the leg-extension degree of freedom is of primary importance to achieving dynamically stable running, and that robust stability may be achieved with minimal compromise of locomotion efficiency.**

I. INTRODUCTION

Robotic legged locomotion is a challenging task due to the complexity of locomotion mechanics. This complexity is a consequence of high system order as well as hybrid nonlinear dynamics that result from intermittent foot-ground contact.

The use of mechanical impedance to control legged robots has been motivated by animal studies. Animals of many sizes and leg layouts have been observed to walk and run using spring-like interactions with the ground [1] and it has been suggested that this spring-like interaction reduces the cognitive load required for robust locomotion [2]. For instance, pre-tuned leg impedance provides an explanation for the fast stabilizing responses to sudden unexpected disturbances observed in cockroaches [3] and appears to account for the body trajectory of running guinea fowl in response to ground-height disturbances [4].

Leg action in biology has historically been termed "spring-like", and a canonical model of running has been the energetically conservative Spring Loaded Inverted Pendulum (SLIP), though actual locomotion systems must have energy dissipation and injection mechanisms to maintain stability [5]. To address this, locomotion control strategies have extended the SLIP model to include automatic energy regulation mechanisms. These strategies include varying the free-length of a spring leg [6]; using a spring leg with viscous damping and hip torque actuation [7] [8]; and using a spring leg with viscous damping and a force source in parallel with the leg [9].

*This work was supported by the DARPA M3 program.
Corresponding author bosworth@mit.edu
[1]Author is with the Department of Mechanical Engineering, Massachusetts Institute of Technology, Cambridge, MA 02139.
[2]Author is with the Department of Brain and Cognitive Science, Massachusetts Institute of Technology.

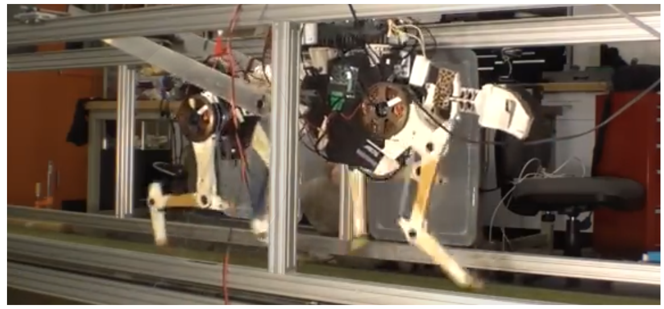

Fig. 1. The MIT Cheetah robot, a machine with actively controllable hip and knee joint, motivates this study of the effect of joint impedance on locomotion performance. The image shows the robot trotting using an impedance control gait described in [17].

A number of robots have used tuned mechanical impedance of the leg joints and simple feedback mechanisms to achieve stable running. Raibert described a family of machines that used the intrinsic mechanical impedance of a pneumatically-driven prismatic leg to hop and run [10]. The Scout [11] and the rHex [12] robots used passive, lightly-damped springy legs and an electric motor at each hip joint. A hexapedal robot, iSprawl, used tuned impedance at the hip joint and tuned axial stiffness in series with feed-forward position profiles of the prismatic leg [13] [14]. Although these robots have demonstrated the effectiveness of tuned leg impedance, how to best select joint impedances for new robots remains an open-ended challenge.

To investigate the effect of leg impedance on locomotion stability and efficiency, this study used a quadrupedal model based on the MIT Cheetah performing the trot gait [15] (Fig 1). The controller commanded individual joint impedances and trajectories, using an approach similar to the first successful trot gaits achieved on the MIT Cheetah [16] [17]. The model included four legs and torso pitch dynamics, in contrast to many model studies that have explored leg impedance, which used a point mass torso and a single leg. These modelling complications were motivated by implementation on the MIT Cheetah robot, where stabilization of pitch dynamics and repetitive footfall patterns were significant challenges to achieving the trot gait. The study focused on sagittal plane locomotion; ongoing research considers more general motion.

This study used exhaustive search of hip and knee impedance parameters to determine their influence on locomotion stability and efficiency. The results show that locomotion stability is most sensitive to selection of knee impedance. The relative importance of knee impedance is demonstrated by analysis of simulation trials during a ground-height disturbance: nearly all variation in limb work during a disturbance response was performed by the knee, not the hip. Experimental data of mechanical work performed in the legs of the MIT Cheetah during a trot gait exhibited joint work patterns similar to the simulation, validating the simulation results. The exhaustive search results also show that, within the range of limb impedance values that result in stable locomotion, limb impedance does not significantly influence locomotion efficiency.

The paper proceeds as follows: Section II describes the rigid body model, the locomotion controller, and the exhaustive search method. Section III presents exhaustive search results and joint work performed by individual simulation and robot trials. Section IV summarizes the findings and implications of the study.

II. METHODS

A. Modeling

This study was performed on a simplified model of the MIT Cheetah robot. The joint layout and mass distribution of the quadrupedal model are shown in Fig 2. The model consisted of a rigid torso constrained to the sagittal plane with four legs of non-zero mass. Given that the action of the knee is to extend the foot relative to the hip, each limb was modeled as a rotating hip joint with a prismatic leg. This approach served to simplify the equations of motion without compromising the relevance of the simulation. The hip and knee joints were assumed to be ideal force sources with a maximum force and speed limit. The model parameters, shown in Table I, approximated the MIT Cheetah robot.

The simulation model and control system were written in the Python programming language. The rigid body dynamics were performed using Open Dynamics Engine (ODE) [18] with an integration time step of 40 μs. The foot-ground contact was modeled with a stiffness and damping of 100 MN/m and 1 MNs/m. A no-slip foot-ground contact condition was specified in the simulation; ground reaction forces and required friction cones were monitored and simulations with friction cone violations were discarded.

B. Controller

Each leg was controlled using only local joint impedance commands and position trajectories, as in the implementation of the trot gait on the MIT Cheetah robot [16][17]. As the joint actuators were considered to be ideal within the torque and speed limits, joint stiffness and damping was commanded directly using proportional gains on the position and velocity feedback [19]; accurate limb impedance has been demonstrated on the MIT Cheetah [20].

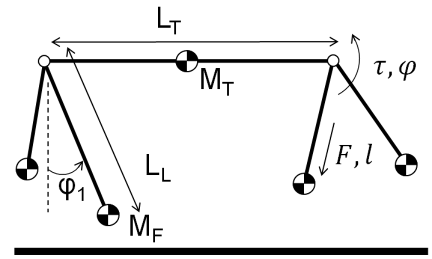

Fig. 2. Schematic of the model. It consisted of a rigid torso with a mass *Mt* and a foot mass *Mf*. Each leg contained a powered rotating hip with position ϕ and commanded torque τ as well as a powered prismatic leg with length *l* and commanded force *F*. The model was constrained to the sagittal plane.

TABLE I

PARAMETERS OF THE MODEL, DERIVED FROM THE MIT CHEETAH

Property	Symbol	Value	Unit
Torso mass	M_T	30	kg
Foot mass	M_F	0.1	kg
Leg free length	L_L	0.5	m
Torso length	L_T	0.65	m
Leg moment	J_L	0.025	kg m^2
Torso moment	J_t	1	kg m^2
Max hip torque	τ_{max}	36	Nm
Max hip speed	$\dot{\phi}_{max}$	50	rad/s
Max knee force	F_{max}	1000	N
Max knee speed	$\dot{l}_{max}$	5	m/s

This study focused on the impedance of the leg during stance. The stance leg control is shown schematically in Fig 3. During the stance phase, the knee impedance and leg-length command were constant, thus the knee joint operated as a passive impedance [21]. The hip joint executed a constant velocity position trajectory described in Eq 1, where commanded hip position ϕ_c was a function of the stance time t_s and commanded hip velocity $\dot{\phi}_c$. The stance clock t_s was reset to zero at the beginning of each stance phase.

$$\phi_c(t) = \dot{\phi}_c t_s \qquad (1)$$

The stance controller began with the knee fully extended and the hip at the commanded stance entrance angle with respect to the body. While a leg was in flight, the stance controller was triggered when the foot was 5 cm from the ground. This enabled swing leg retraction to precede the contact event [22]. The ground height trigger value was selected by trial and error.

All trials used identical swing leg controllers which for brevity are not discussed in depth. Swing leg control consisted of four discrete states which proceeded sequentially to perform leg lift-off and return actions. The swing leg control operated within the workspace of the MIT Cheetah robot; all control actions maintained the joint torque and speed requirements described in Table I.

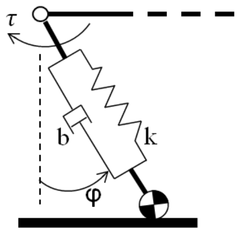

Fig. 3. Schematic of the stance leg controller. The controller consisted of a passive knee impedance (stiffness k and damping b) and hip torque τ. The hip torque was controlled by a constant velocity position trajectory command ϕ_c (Eq 1) with commanded hip stiffness and damping.

C. Exhaustive Search: the Stance Leg Parameter Space

Exhaustive search of the stance leg control parameters was performed to identify the effect of joint impedance on locomotion stability and efficiency. In the exhaustive search, a simulation trial was performed for every combination of parameter values tested, which are shown in Table II.

A simulation trial consisted of trotting on flat ground at about 3 m/s, and operating over a 2.5 cm ground height disturbance. An animation of trotting over the ground height disturbance is shown in Fig 4. A trial began with the machine in flight moving forward with a velocity of 3 m/s. The commanded stance hip velocity was 7 rad/s, which combined with the leg free-length of 0.5 m (see Table I), corresponded to forward velocities of about 3 m/s. The ground height disturbance was introduced at the twentieth stride. This number of strides was found to be a conservatively adequate time for stable gaits to settle into a limit cycle before the disturbance. Step-down trials were easier to perform than step-up trials as they avoided tripping or foot scuffing. When tripping was avoided, simulations showed similar responses to both disturbances.

A brief discussion of the joint impedance values chosen for analysis is provided. All parameter ranges started from zero magnitude. The knee stiffness range was selected to include, and exceed, the values of leg stiffness observed in biological systems of similar size [1]. A wide range of knee damping values was chosen; values above the maximum shown in this study did not result in successful locomotion trials. The maximum hip stiffness and damping values were limited by joint saturation: values of hip impedance approaching and exceeding the range described in Table II would not be consistently realizable on the MIT Cheetah hardware.

The entrance angle of the hip during the stance control was selected to be 0.5 radians; the commanded exit angle was also 0.5 radians, though leg lift-off control could begin if excessive friction cone violations were imminent. The entrance and exit angles were selected using exhaustive search results not reported here, observation of individual simulation trials, and observations of hip kinematics from studies of biological systems [1]. Trends in the reported exhaustive search results were identical for a wide range of entrance and exit angle kinematics.

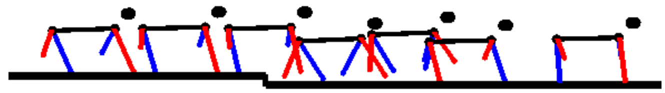

Fig. 4. The exhaustive search simulation trials consisted of trotting on flat ground and over a single ground height disturbance of 2.5 cm. An animation of a successful trotting trial is shown here. The red and blue legs correspond to the left and right side of the robot, respectively; in a trot, diagonal pairs of legs interact with the ground simultaneously.

TABLE II

JOINT IMPEDANCE VALUES USED IN THE EXHAUSTIVE SEARCH

Parameter	Range of values	Unit
Hip stiffness	[0, 5, 25, 50, 75, 100, 150, 200, 300]	Nm/rad
Hip damping	[0, 5, 25, 50, 75, 100, 150, 200, 300]	Nms/rad
Knee stiffness	range(0,12000,1000)†	N/m
Knee damping	range(0,320,40)	Ns/m

†Defines an array using *range(start,stop,step)* notation, taken from the Python programming language.

D. Exhaustive Search: Locomotion Performance Metrics

This section describes the performance metrics used to organize the results of the exhaustive search trials. Table III describes the performance criteria used to deem an individual trial as successful; trials that were unsuccessful were discarded from the results described in the following sections.

Metrics of performance included measures of locomotion stability, energetic efficiency, and important physically reasonable gait criteria. The metrics are discussed in the subsections below.

1) Locomotion stability: Locomotion stability was assessed by measuring the state of the torso at a repeating point in the gait cycle; the state of the torso when the rear left leg lifted off of the ground was used. The lift-off state of the torso consisted of the forward velocity, vertical height, vertical velocity, pitch angle, and pitch angle rate.

In the flat ground trials, the magnitude of the standard deviation of the lift-off state was used to evaluate whether a limit cycle had been achieved. The lift-off state was measured and the standard deviations of the complete trial were calculated during each stride. Results from the first

TABLE III

PERFORMANCE CRITERIA USED TO ASSESS SIMULATION TRIALS OF THE EXHAUSTIVE SEARCH STUDY.

Property	Value
Settling time	3 strides maximum
Standard deviation of lift-off torso height	100 μm maximum
Friction cone validity	98% maximum
Leg pair force balance	3% maximum
Stride frequency	4.5 Hz maximum
Average forward velocity	2 m/s minimum

20 strides were discarded to ensure the machine had ample opportunity to settle into a limit cycle.

In the ground height disturbance trials, the lift-off state of the machine was logged for each stride after application of the disturbance. Each of the five torso states s_n were weighted equally in the creation of a single lift-off value *V*, which was calculated for each *i*'th step as in Eq 2.

$$V_i = \sqrt{\sum_{n=0}^{4} \left(\frac{s_{n,i}}{s_{n,cycle}} \right)^2} \tag{2}$$

The final lift-off state of a trial was considered to approximate the fixed point of the limit cycle $s_{n,cycle}$. The settling time was defined as the number of strides after the ground height disturbance before the lift-off value *V* settled to within +/- 5% of its final value.

2) Energetic efficiency: The mechanical cost of transport C_t was used to measure the energetic efficiency of each trial. The cost of transport is the ratio of the positive actuator work *W* to the product of distance travelled *d*, machine mass *m*, and gravity g.

$$C_t = \frac{W}{mgd} \tag{3}$$

This measure is commonly used to evaluate gaits across actuator types because it only considers mechanical power, excluding other energy losses associated with mechanical power production. The mechanical cost of transport excludes important energy flows in the MIT Cheetah hardware such as, motor heat dissipation, joint friction and regenerative power but was chosen for generalizability.

3) Physically realistic constraints: The other performance criteria described in Table III pertained to physical requirements of a reasonable trot gait that were not fully captured by the initial modeling assumptions and constraints. Friction cone validity was measured as the percentage of time steps in which the vertical ground reaction force exceeded the horizontal force, presuming a unity magnitude coefficient of friction. The leg pair force balance was measured as the ratio between the total vertical ground reaction forces exerted by the left and right side of the robot during the simulation trial. Although the model was constrained to the sagittal plane, it was presumed that a good trot gait should have balanced loading in the transverse plane. The maximum stride frequency requirement was included as a result of observations of the practical limit of swing leg accelerations in the MIT Cheetah. A minimum average forward velocity was included to remove very slow gaits from consideration.

III. RESULTS AND DISCUSSION

A. Sensitivity of Leg Impedance Parameters to Stability and Efficiency

In the exhaustive search, a simulation trial was performed for every combination of parameter values studied (see Table II), thus each individual value of a parameter of interest was tested with the same combinations of other parameters.

The relationship between parameter values and system stability was found by tabulating the number of successful gaits achieved for each individual parameter value (using the criteria contained in Table III); Fig 5(a) shows a histogram of successful gaits for each parameter value studied. The data shows that locomotion performance was sensitive to values of knee stiffness and damping, as most successful trials clustered in a narrow range of these values. The success of simulation trials was also dependent on hip damping, though to a lesser extant than the knee impedance values; zero hip damping resulted in minimal locomotion success, and a peak value of damping had nearly twice as many successful gaits than higher damping values. Alternatively, the value of hip stiffness had minimal effect on the likelihood of a successful trial.

The relationship between parameter values and energetic efficiency was found by averaging the energetic cost of transport (Eq 3) of the successful gaits achieved for each individual parameter value; the result is shown in Fig 5(b). Energetic cost varied by almost a factor of two through all of the trials, though when constrained to the window of particularly robust parameter values, the dynamic range of energetic cost was very low. This result shows that, within the span of stable gaits, energetic efficiency is not sensitive to joint impedance.

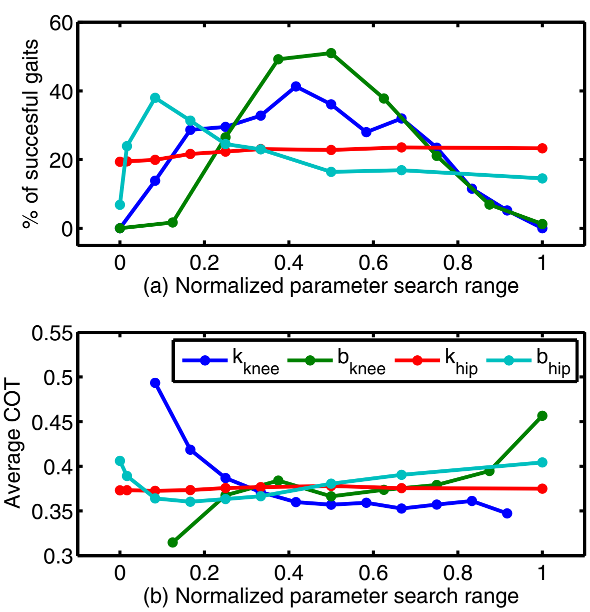

Fig. 5. Results of the exhaustive search trials, normalized between 0 and 1 for each range of values tested (see Table II). (a.) The number of successful gaits achieved for each individual parameter value in the parameter search, expressed as the percentage of all parameter combinations tested. Low numbers of successful gaits show that few parameter combinations achieved successful locomotion with the corresponding parameter; high numbers show that many gaits were successful with a given parameter. Large dynamic range across parameter values shows that stability performance is sensitive to the parameter being considered. (b.) The average cost of transport (COT) for the successful gaits of the exhaustive search. Note that the high and low values associated with knee impedance parameters are in regions of low success rate as seen in (a.).

B. Actuator Work During Simulation of Ground Height Disturbance

Actuator worked performed by the leg joints during the ground height disturbance was analyzed to investigate why stability was more sensitive to knee impedance than hip impedance.

Fig 6 shows the ground reaction forces and hip and knee joint actuator power for all four legs of the model during a ground height disturbance of 2.5 cm. The data shows cyclic force and power profiles disrupted by the disturbance. In the disturbance response, nearly all of the variation in actuator work was performed in the knee joint; the hip joint work profile is nearly identical to its limit cycle profile.

In the trial shown, the hip joints performed positive work, while the knee joints performed more negative work than positive work. Simulation trials with zero or low leg damping resulted in nearly equal ratios of positive and negative knee work, though these trials stabilized poorly; an observation consistent with the exhaustive search results, which show poor performance with low values of knee damping.

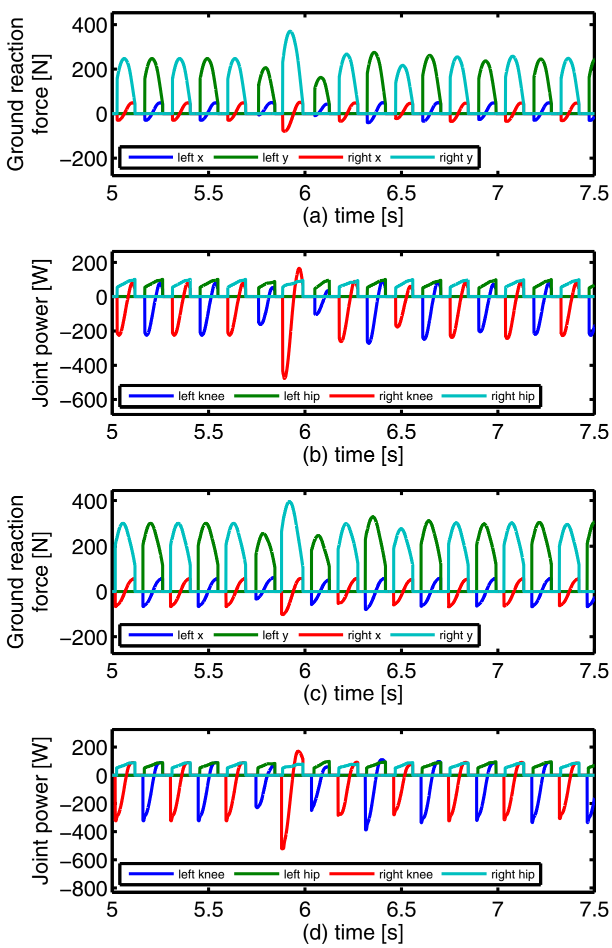

Fig. 6. Simulation trial of the robot's response to ground height disturbance. The ground height disturbance began at t = 5.75 s. (a.) Ground reaction forces of the front leg; (b.) Actuator power in the front leg joints during stance; (c.) Ground forces of the rear leg; (d.) Actuator power in the rear leg joints.

The trial shown in Fig 6 had a hip stiffness of 100 Nm/rad, hip damping of 5 Nms/rad, knee stiffness of 5000 N/m, and knee damping of 100 Ns/m — values identical to the controller used to implement the trot gait on the MIT Cheetah reported in [17]. Numerous simulations were analyzed; in fast-settling gaits, variations in work during the disturbance response were predominantly performed in the knee joint.

C. Actuator Work on the MIT Cheetah Robot and the Simulation Model During Steady Running

Fig 7 shows the mechanical power in the knee and hip joints of the MIT Cheetah robot and simulation model, while trotting at approximately 3 m/s over two strides.

The experimental data of the MIT Cheetah were acquired during trials that are further described in [17]. The joint work data of the MIT Cheetah was assembled from measurements of commanded motor torques and angles; the work at the hip and articulated knee joints were calculated using the motor data and the leg Jacobian. Though not identical, the model and hardware controllers were similar: each of the trials used a fixed, cyclic position trajectory and constant mechanical impedance for each leg; each used commanded hip impedance of 100 Nm/rad and 5 Nms/rad, and knee impedance of 5000 N/m and 100 Ns/m; each used similar stance-state entrance and exit angles and a nearly constant radial leg length command during stance.

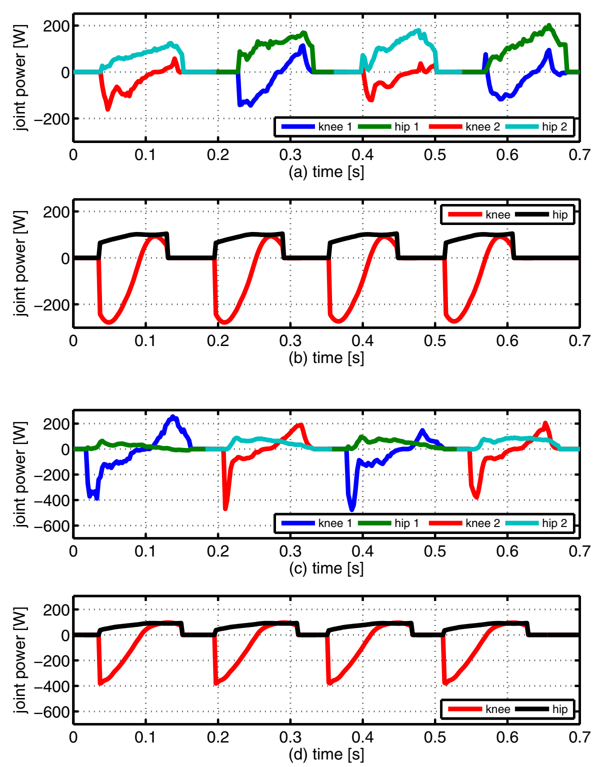

Fig. 7. Joint power as a function of time for the MIT Cheetah robot and the simulation model. (a.) front legs of the MIT Cheetah; (b.) front legs of the model; (c.) rear legs of the MIT Cheetah; (d.) rear legs of the model. In the simulation model, the left and right legs performed identical actions in steady state. Experimental MIT Cheetah data is provided by [17].

The data shows similarity in the curve shapes and magnitudes of positive and negative work performed in the hip and knee joints. The cumulative positive and negative joint work of the robot hardware and model are shown in Table IV; this tabulation accounts for an estimated 15% loss in power transmission through the gearbox of the hardware motors. The largest discrepancy is in the negative work performed in the knee: the simulation trial performed nearly 1.5 times more negative knee work. Both hardware and simulation trials performed more negative knee work than positive knee work. The reduced negative actuator work in the robot trial may be due to additional dissipation in the drive-train and during the foot-ground impact event. Differences in the controller implementation as well as differences in leg morphology may also account for some of the disparity. Although further testing of the MIT Cheetah robot should be performed, this preliminary model-experiment agreement provides further validation of the explanation of the roles of the hip and knee joints in maintaining locomotion stability in an impedance control gait.

TABLE IV
JOINT WORK [J] PERFORMED BY THE MIT CHEETAH ROBOT AND SIMULATION DURING THE TROT GAIT.

Joint	MIT Cheetah Robot	Simulation
positive hip work	58.6	70
negative hip work	0.2	0
positive knee work	21.2	27.5
negative knee work	60.8	94

IV. CONCLUSIONS

This study investigated the effect of hip and knee impedance on locomotion stability and efficiency during quadrupedal trotting. Results of an exhaustive search of impedance parameters showed that locomotion stability is sensitive to both knee stiffness and damping, and insensitive to hip impedance. Analysis of individual simulation trials provides an explanation for the sensitivity to knee impedance: During response to a ground-height disturbance, nearly all variations in the actuator work were performed by the knee joint. The simulation model was based on the MIT Cheetah robot; experimental data of the MIT Cheetah showed similar joint work trends to the simulation results. The exhaustive search also revealed that joint impedance values did not have a significant effect on the mechanical cost of transport. These results indicate that the dynamic response of the leg-extension degree of freedom is of primary importance to achieving dynamically stable running, and that robust stability may be achieved with minimal compromise of locomotion efficiency.

ACKNOWLEDGMENT

The authors thank the MIT Biomimetic Robotics Laboratory, in particular Dr. Dong Jin Hyun, for generating the data of the MIT Cheetah used in this report.

This project was supported by the DARPA Maximum Mobility and Manipulation (M3) Program.

REFERENCES

[1] Farley, Claire T., James Glasheen, and Thomas A. McMahon. "Running springs: speed and animal size." Journal of experimental Biology 185.1 (1993): 71-86.
[2] Full, Robert J., and Daniel E. Koditschek. "Templates and anchors: neuromechanical hypotheses of legged locomotion on land." Journal of Experimental Biology 202.23 (1999): 3325-3332.
[3] Full, R. J., Autumn, K., Chung, J. I., & Ahn, A. (1998). Rapid negotiation of rough terrain by the death-head cockroach. American Zoologist, 38(5), 81A.
[4] Daley, M. A., Usherwood, J. R., Felix, G., & Biewener, A. A. (2006). Running over rough terrain: guinea fowl maintain dynamic stability despite a large unexpected change in substrate height. Journal of Experimental Biology, 209(1), 171-187.
[5] Ahn J, Hogan N (2012) A Simple State-Determined Model Reproduces Entrainment and Phase-Locking of Human Walking. PLoS ONE 7(11): e47963. doi:10.1371/journal.pone.0047963.
[6] Schmitt, J., and J. Clark. "Modeling posture-dependent leg actuation in sagittal plane locomotion." Bioinspiration & biomimetics 4.4 (2009): 046005.
[7] Ankarali, M. Mert, and Ulu Saranli. "Stride-to-stride energy regulation for robust self-stability of a torque-actuated dissipative spring-mass hopper." Chaos: An Interdisciplinary Journal of Nonlinear Science 20.3 (2010): 033121.
[8] Jun, Jae Yun, and Jonathan E. Clark. "Dynamic stability of variable stiffness running." Robotics and Automation, 2009. ICRA'09. IEEE International Conference on. IEEE, 2009.
[9] Cham, Jorge G., and Mark R. Cutkosky. "Dynamic stability of open-loop hopping." Journal of dynamic systems, measurement, and control 129.3 (2007): 275-284.
[10] Raibert, M. H. (1985). Legged robots that balance.
[11] Poulakakis, I., Smith, J., & Buehler, M. "Modeling and experiments of untethered quadrupedal running with a bounding gait: The Scout II robot." The Int J of Rob Res 24.4 (2005): 239-256.
[12] Altendorfer, R., ..., & Koditschek, D. E. (2001). RHex: a biologically inspired hexapod runner. Autonomous Robots, 11(3), 207-213.
[13] Cham, J. G., ... , & Cutkosky, M. R. (2004). Stride period adaptation of a biomimetic running hexapod. The Int J of Rob Res, 23(2), 141-153.
[14] Kim, S., Clark, J. E., & Cutkosky, M. R. (2006). iSprawl: Design and tuning for high-speed autonomous open-loop running. The International Journal of Robotics Research, 25(9), 903-912.
[15] S. Kim. Cheetah-inspired quadruped: High-speed locomotion platform. Jun. 11, 2013. [Online]. Available: http://biomimetics.mit.edu:8100/wordpress/
[16] Falconer J, MIT Cheetah Robot Runs Fast, and Efficiently. IEEE Spectrum. Posted 14 May 2013. [online] http://spectrum.ieee.org/automaton/robotics/robotics-hardware/mit-cheetah-robot-running. Accessed June 11 2013.
[17] Hyun D., Seok S., Lee J., and Kim S., "High Speed Trot-running: Implementation of a Hierarchical Controller using Proprioceptive Impedance Control on the MIT Cheetah." (under review).
[18] Smith, R.: ODE: Open Dynamics Engine
[19] Hogan, N. (1984, June). Impedance control: An approach to manipulation. In American Control Conference, 1984 (pp. 304-313). IEEE.
[20] Seok, S., Wang, A., Otten, D., & Kim, S. (2012, October). Actuator design for high force proprioceptive control in fast legged locomotion. In 2012 IEEE/RSJ IROS (pp. 1970-1975).
[21] Colgate, E., & Hogan, N. (1989, May). An analysis of contact instability in terms of passive physical equivalents. In Robotics and Automation, 1989. Proceedings., 1989 IEEE International Conference on (pp. 404-409). IEEE.
[22] Seyfarth, A., Geyer, H., & Herr, H. (2003). Swing-leg retraction: a simple control model for stable running. Journal of Experimental Biology, 206(15), 2547-2555.